Received: 29 January 2020 | Revised: 10 March 2020 | Accepted: 3 April 2020

DOI: 10.1002/jmr.2852

RESEARCH ARTICLE

Journal of Molecular Recognition WILEY

A novel bioassay for the monitoring of carcinoembryonic antigen in human biofluid using polymeric interface and immunosensing method

Mahbubeh Moradkhani[1,2,3] | Fatemeh Farshchi[4,5,6†] | Mohammad Hasanzadeh[7] | Ahad Mokhtarzadeh[8]

[1]Food and Drug Safety Research Center, Tabriz University of Medical Sciences, Tabriz, Iran

[2]Department of Biochemistry, Higher Education Institute of Rab-Rashid, Tabriz, Iran

[3]Biotechnology Research Center, Tabriz University of Medical Sciences, Tabriz, Iran

[4]Nutrition Research Center, Faculty of Medicine, Tabriz University of Medical Sciences, Tabriz, Iran

[5]Liver and Gastrointestinal Diseases Research Center, Tabriz University of Medical Sciences, Tabriz, Iran

[6]Hematology-Oncology Research Center, Tabriz University of Medical Sciences, Tabriz, Iran

[7]Pharmaceutical Analysis Research Center, Tabriz University of Medical Sciences, Tabriz, Iran

[8]Immunology Research Center, Tabriz University of Medical Sciences, Tabriz, Iran

Correspondence
Mohammad Hasanzadeh, Pharmaceutical Analysis Research Center, Tabriz University of Medical Sciences, Tabriz, Iran.
Email: hasanzadehm@tbzmed.ac.ir, mhmmd_hasanzadeh@yahoo.com

Funding information
Tabriz University of Medical Science

Abstract

Carcinoembryonic antigen (CEA) is a member of a family of cell surface glycoproteins. Recognition of CEA is needed to monitor the physiological status of the patient for treatment and also it is important to assess the severity of the disease. In this work, we reported a novel sandwich-type electrochemical immunosensor based on gold nanoparticles functionalized cysteamine-glutaraldehyde (AuNPs-CysA-GA) and it successfully designed to detection of the CEA biomarker in a human plasma sample. The AuNPs-CysA-GA provides a large surface area for the effective immobilization of CEA antibody, as well as it ascertains the bioactivity and stability of immobilized CEA antigens. Biotinylated-anti-CEA antibody (Ab1) was immobilized on the surface of glassy carbon electrode (GCE) modified AuNPs-CysA-GA. Also, secondary antibody (HRP-Ab2) was costed immobilized to complete the sandwich part of immunosensor. Field emission scanning electron microscope (FE-SEM and EDS), was employed to monitor the sensor fabrication procedure. The immunosensor was used for the detection of CEA using differential pulse voltammetry (DPVs) technique. The proposed interface led to enhancement of accessible surface area for immobilizing high amount of anti-CEA antibody, increasing electrical conductivity, boosting stability, and biocompatibility. Finally, the low limit of quantitation (LLOQ) of the proposed immunosensor was obtained as 7 ng/mL with the linear range of 0.001-5 μg/L. The proposed immunoassay was successfully applied for the monitoring of the CEA in unprocessed human plasma samples. Obtained results paved that the proposed bioassay can be used as a novel bioassay for the clinical diagnosis of cancer based on CEA monitoring.

KEYWORDS

biomedical analysis, biosensor, carcinoembryonic antigen (CEA), sandwich type immunosensor; polymer matrices

1 | INTRODUCTION

Cancer is one of deadly diseases in the world. Cancer is a group of diseases that is associated with abnormal cell growth, with the possibility

[†]Co-first author: Equal contribution.

of attack or spread to other parts of the body. This contrasts with benign tumors, which does not spread.[1] Possible signs and symptoms include a mass, abnormal bleeding, prolonged cough, unexplained weight loss, and changes in bowel movements. Although these symptoms may indicate cancer, they can have other causes.[2] More than 100 types of cancer affect humans.[1] Usually, the most of cancers with 90%-95% of cases are reason by genetic mutations from environmental factors, while the remaining 5%-10% are attributed to hereditary genetics.[3] A cancer related biomarker, a substance or process that it indicates cancer in the body. Perhaps a molecule secreted by a tumor or a special reply of the body is overexpressed because of cancer incidence and growth.[4] The development of an efficient diagnostic procedure for diagnosis of cancer, Development, and monitoring of treatment effectiveness, is an important bio-analytical goal.[5]

Biomarkers are classified according to their chemical nature to DNA, RNA, and proteins and are classified as prognostic and diagnostic by disease level.[6] Biomarkers play an important role and through diagnosis are used for staging and ordering of tumor/cancer, and during prognosis.[7]

With the development of proteomics, serum tumor markers, such as carcinoembryonic antigen (CEA), alpha fetoprotein, CA125, CA19-9, and cytokeratin 19 fragment, have been widely used as screening tools for risky crowd people in yearly medical examinations.[8]

CEA is a 180 kDa glycoprotein and it is provided as a tumor marker to appraise the reply to treatments of cancers for example breast tumors, cervical carcinomas, colon tumors, and ovarian carcinoma.[9,10] It has interposition in cell adhesion and continuously over expressed in cancer. In a healthy person, the normal range of CEA concentration in an adult is less than 5 ng/mL.[11]

In the context of the minimal presence of CEA in biological specimen, it is essential to gain a high accuracy detection method in clinical tumor diagnosis and prognosis.[12,13] Some of methods have been developed to detection of CEA, such as the enzyme-linked immunosorbent assay (ELISA),[14] the electrochemical immunoassay,[15] fluorescence,[16] and electrochemical assays.[17]

Although ELISA based methods are common, but these techniques are costly and need to export operator. Therefore designed of a simple, sensitive, also economical method for detection of CEA is required.[18]

A biosensor is an analytical device used to detect chemicals substance and combines a biological compound with a physicochemical detector.[19-25] Immunosensors are compact analytical devices in which the occurrence of the formation of antigen-antibody complexes is identified and converted by means of a transducer to an electrical signal that can be processed, recorded, and displayed.[21] Sandwich-type electrochemical biosensors are more selective and sensitive, and appropriate for detection of tumor biomarker. To reach a high efficient immunosensor new modification on the structure of immunosensor is necessary.

Signal amplification related to the use of nanoparticle amplification labels and the formation of nanoparticle-biomolecule assemblies provides the basis for sensitive electrical and optical detection. Such procedures couple the extensive features of NP-biomolecule associations with sensitive electrochemical or optical transduction. Gold nanoparticles (AuNPs) have been widely used in biotechnology because of their unique properties and multiple surface properties. AuNP provides a versatile substrate for the immobilization of biological agents such as oligonucleotides, antibody, and protein.[25] AuNPs are also become promising candidates in the design of new biological materials for biomedical analysis.[25] The versatility of AuNPs has provided useful materials for a wide range of biomedical applications. In diagnostics, the binding event between the analytes and AuNPs can alter the physicochemical properties of AuNPs, resulting in detectable signals.[26] Sensitive overlapping ligands on AuNPs (citrate, thiol or other adsorbed ligands) can be displaced by the thiols by the site-ligand exchange reaction to synthesize protected AuNPs with a mixed layer.[27] The ligand exchange site allows the secondary binding of organic molecules or biomolecules to the surface of AuNPs.[27] Noncovalent conjugation is an easier way to bind molecules to AuNPs because they can attach through various interactions, such as through specific binding affinity, electrostatic interactions, and hydrophobic interactions.[28] Noncovalent interactions are widely used in delivery and measurement areas due to their ease of release and reversible nature. On the other hand, the covalent conjugation of molecules with AuNPs stabilizes the conjugation, which is more useful when stable structures are required.[29] Cysteamine (CysA) (2,2′-dithiobisethanamine) is an organic disulfide formed by Cys warming resulting from decarboxylation. It is often used as a sulfhydryl reagent, enzyme inhibitor, and radiation-protective agent. Also, mussel-inspired chemistry is a useful method for the fabrication of functional composites with various applications in biomedical and environmental fields. So, this is a new technique for the fabrication of sensors.[30-40] But, electrochemical fabrication is so interesting method for the sensor fabrication.[29,41-45]

In this study, application of AuNPs as a new matrix for providing excellent substrate to immobilize bio-recognition (Antibody) element toward monitoring of CEA in human bio fluids has been utilized. To the best of our knowledge, the fabrication of AuNPs-CysA-GA on the electrode surface and its application for the preparation of electrochemical immunosensors toward detection of CEA were initially reported in this work. In this study, we reported a novel sandwich-type electrochemical immunosensor based on gold nanoparticles functionalized Cysteamine and glutaraldehyde (AuNPs-CysA-GA) and it successfully designed to detection of the CEA biomarker in a human plasma sample. The AuNPs-CysA-GA provides a large surface area for the effective immobilization of CEA antibody, as well as it ascertains the bioactivity and stability of immobilized CEA antigens. Biotinylated-anti-CEA antibody (Ab1) was immobilized on the surface of glassy carbon electrode (GCE) modified AuNPs-CysA-GA, secondary antibody (HRP-Ab2) was costed immobilized to complete the sandwich part of immunosensor. Field emission scanning electron microscope (FE-SEM and EDS), was employed to monitor the sensor fabrication procedure. The immunosensor was used for the detection of CEA using differential pulse voltammetry (DPVs) technique. The proposed interface led to enhancement of accessible surface area for immobilizing high amount of anti-CEA antibody, increasing electrical conductivity, boosting stability and biocompatibility. Finally, the low limit of

quantitation (LLOQ) of the proposed immunosensor was obtained as 7 ng/mL which this evaluation was performed at linear range of 0.001-5 μg/L. The proposed immunoassay was successfully applied for the monitoring of the CEA in unprocessed human plasma samples. Obtained results paved that the proposed bioassay can be used as a novel bioassay for the clinical diagnosis of cancer based on CEA monitoring.

2 | EXPERIMENTAL

2.1 | Reagents and materials

Human CEA ELISA kit including CEA antigen, biotinylated antibody (anti-CEA) (HRP Labeled anti CEA), standard buffer, and dilute solutions were obtained from Can Ag Diagnostic AB Technology Co., (Gothenburg, Sweden). Potassium ferrocyanide $K_4Fe(CN)_6$, potassium ferricyanide $K_3Fe(CN)_6$, hydrochloric acid, citric acid, ammonia, $Fecl_3.6H_2O$, $FeSO_4.7\ H_2O$, glutaraldehyde, bovine serum albumin (BSA), 1-ethyl-3-(3- dimethylaminopropyl) carbodiimide hydrochloride (EDC), N-hydroxysuccinimide (NHS), cysteamine hydrochloride, hydrogen tetrachloroaurate(III)hydrate ($HAuCl_4{\cdot}3H_2O$), were obtained from Sigma-Aldrich (Ontario, Canada). Phosphate buffer saline (PBS) solution (0.05 M) was prepared by Na_2HPO_4 (0.1 M) and NaH_2PO_4 (0.1 M) with 0.15 M of NaCl in deionized water. Human plasma samples were obtained from the Iranian Blood Transfusion Research Center (Tabriz, Iran).

2.2 | Apparatus and electrochemical measurement

Electrochemical measurements were performed by using a computer-controlled electrochemical system comprising of AUTOLAB system with PGSTAT302N (Eco Chemie, Utrecht, The Netherlands) using NOVA 1.11 software. The conventional three-electrode electrochemical cell was set using GCE, Ag/AgCl, and a platinum wire as the working, reference, and counter electrode, respectively. The surface morphology of the materials and interfaces was evaluated by FE SEM (field emission scanning electron microscopy) which was conducted on a TESCAN system of FEG-SEM MIRA3 TESCAN (Brno, Czech Republic). The elemental analysis of the electrode surface was done by energy dispersive spectroscopy (EDS) of MIRA3 TESCAN (Brno, Czech Republic) model.

2.3 | Fabrication of immunosensor

First, GCE electrode was inserted into acetone and subsequently to the 1% solution of H_2SO_4 to remove the possible organic and inorganic impurities. Then, GCE working electrodes was modified by AuNPs. For this purpose, 6 mM of $HAuCl_4$ was mixed with 0.1 M of KNO_3. In the next step, this solution magnetically stirred for an hour.

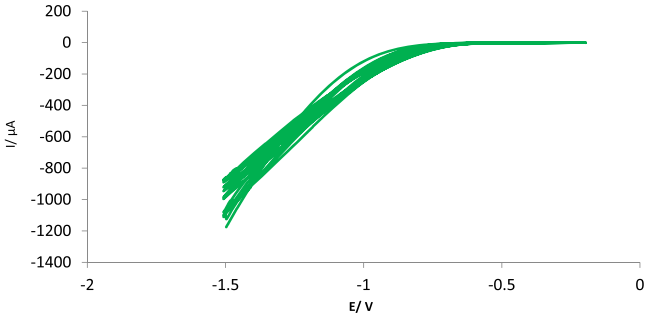

FIGURE 1 CVs of GCE electrode on the solution of $HAuCl_4$ (6 mM) + KNO_3 0.1 M. Scan rate is 100 mV/s, Number of cycle = 10 cycle

Then, the solution was transformed to electrochemical cell. Finally, cyclic voltammograms were recorded in 10 cycles and a potential range of −1.5 to 0.2 V which scan rate was 100 m V/s.

The results from cyclic voltammograms were shown in Figure 1 which reveals the successful electrodeposition of AuNPs on the surface of GCE electrode.

The second step consisted of treatment in CysA for 1 hour. CysA functionalized (AuNPs) were found more suitable for immunosensor application. CysA and AuNPs covalently interact with each other via formation of a covalent bond between the sulfur group of CysA and AuNPs. Subsequently, CysA capped AuNPs provide free amine group for interaction with a carboxylic group of Fc region of antibody via a covalent bond, then the surface of modified electrode incubated for 1 hour with glutaraldehyde which worked as a crosslinking in this step.

After preparation of this interface, biotinylated anti-CEA antibody (Ab1) mixed with EDC/NHS and incubated on CysA-AuNPs-GA/GCE electrode and placed in 4°C for 3 hours. Then in purpose of blocking incubated anti-CEA antibody, CysA-AuNPs-GA/Ab1/GCE electrode immersed in BSA solution for 1 hour. Afterwards, CEA antigen incubated on the surface of prepared electrode (CysA-AuNPs-GA/Ab1/BSA/GCE), and placed in 4°C for 4 hours. Subsequently, 10 μL of anti-CEA antibody-HRP(Ab2) solution was immobilized on the surface of CysA-AuNPs-GA/Ab1/BSA/CEA/GCE for further 60 minutes. Finally, the electrochemical properties of the sandwich-type immunosensor were evaluated by DPV. It should be noted that after all incubation steps, the electrodes were washed by standard buffer solution. The preparation procedure of the sandwich-type electrochemical immunosensor is illustrated in Scheme 1.

2.4 | Morphology and elementary analysis of the synthesized interface and bio device

After preparation of the immunosensor, microscopic evaluation of the surface was investigated by FESEM. Figure S1A-F shows the FE-SEM

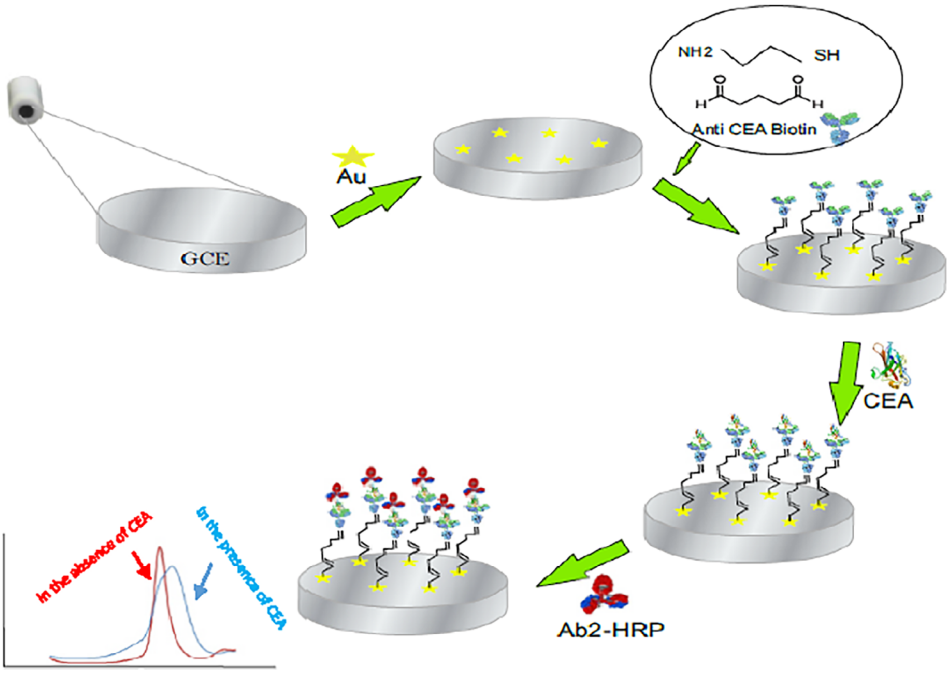

SCHEME 1 Fabrication procedure of the sandwich-type electrochemical immunosensor for detection of CEA

images of AuNPs/GCE (A), AuNPs-CysA/GCE (B), AuNPs-CysA-GA/GCE (C), AuNPs-CysA-GA/Ab1/GCE (D), AuNPs-CysA-GA/Ab1/CEA/GCE (E), AuNPs-CysA-GA/Ab1/CEA/Ab2/GCE (F) electrodes.

FE-SEM images have a high magnification surface that represents AuNPs on the GCE electrode surface which proves the specialty of AuNPs, in increasing the surface of electrode. It is important to point out that, after incubation of AuNPs-CysA-GA electrode with the antibody, the morphology of the electrode surface was changed, indicating a successful coupling between interface and antibodies (Figure S1A-F).

Figure S1A-F show the successful immobilization of antigen and Ab2 on the surface of AuNPs-CysA-GA/Ab1/BSA/GCE electrode. As can be seen after HRP-Ab2 immobilization, morphology of the electrode was changed which confirmed interaction of secondary Ab2 with epitope of CEA.

To confirm obtained results Map Analysis was utilized. The distribution of elements confirms the formation matrices and bio interface.

Also, the Existence of S-P groups on map analysis, confirmed the presence of biological elements (Ab1, CEA, Ab2) on the surface of modified Electrode.

3 | RESULTS AND DISCUSSION

3.1 | Electrochemical behavior of engineered immunosensor

The electrode modification steps were evaluated by DPV technique in 0.01 M $[Fe(CN)_6]^{3-/4-}$ which has been shown in Figure 2. The characteristic peak of bare GCE was markedly increased after its modification with AuNPs, CysA, and GA that might be related to the excellent property of AuNPs, such as high specific surface area and electrical conductivity. Interestingly, the obtained results clearly show that the combination of AuNPs-CysA and Ab definitely alter the nature of DPV oxidation peak current. As can be obtained from DPV, the oxidation peaks current of AuNPs-CysA modified GCE increased in accordance with the increase of the effective surface area. Presence of a highly conductive AuNPs layer on the GCE surface with a large surface area shows a signal amplification for the redox probe, due to the improvement of the electron transfer process. As it is obvious, changes in the current responses are completely distinguishable from DPVs, which highlights the DPV's capability in tracing small changes on this conductive platform in the presence of other reagents compare to the represented voltammograms in the same condition. After adding glutaraldehyde, the peak intensity decreased slightly to 26.7 μA. This indicates that the presence of these nanomaterials increases the geometric surface area.

In the next step, after incubation of Ab1 to the GCE surface modified by AuNPs-CysA-GA, the peak currents were decreased. Insulation of the electrode surface by antibody (Ab1) reduces the efficiency of the electron exchange from the mediator solution, and slows down the kinetics of electron transfer. Ab1 has been successfully immobilized at the modified GCE surface. According to poor conductivity of antibody, the electron transfer occurs at a lower rate. Also, after CEA antigen incubation, the redox peak has been reduced again compared to the previous step, which indicates the successful formation of the antibody-antigen complex. The formation of this immune complex reduces conductivity and limits electron transport. At the next step, after incubation of Ab2-HRP, the electrochemical signals

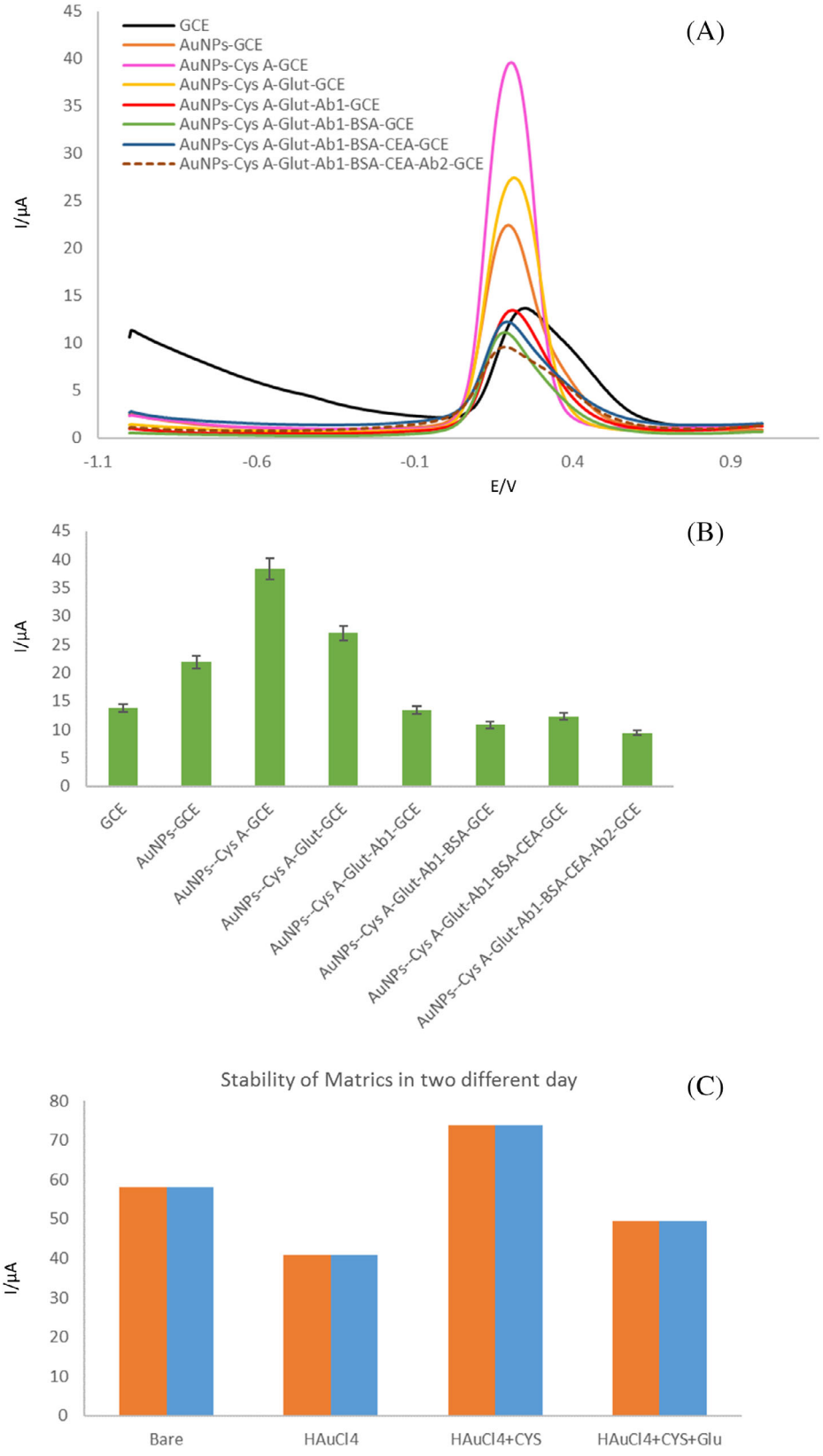

FIGURE 2 DPVs A, of AuNPs, AuNPs-CysA, AuNPs-Cys-GA,AuNPs-CysA-GA/Ab1, AuNPs-CysA-GA/Ab1/BSA, AuNPs-CysA-GA/Ab1/BSA/CEA, AuNPs-CysA-GA/Ab1/BSA/CEA/Ab2 at the surface of GCE electrode. B, Histogram of peak current vs type of electrode. Supporting electrolyte is 1 mM of $[Fe(CN)_6]^{-3/-4}$. C, Histogram of stability of matrices in two different days

were decreased because of hindered electron transfer effect. On the other hand, the antibodies act as an insulter and reduce the electron transfer rate.

3.2 | Kinetic study

Scan rate is one of the effective factors in the evaluation of redox reactions for the analytes detection. Also, using the relationships

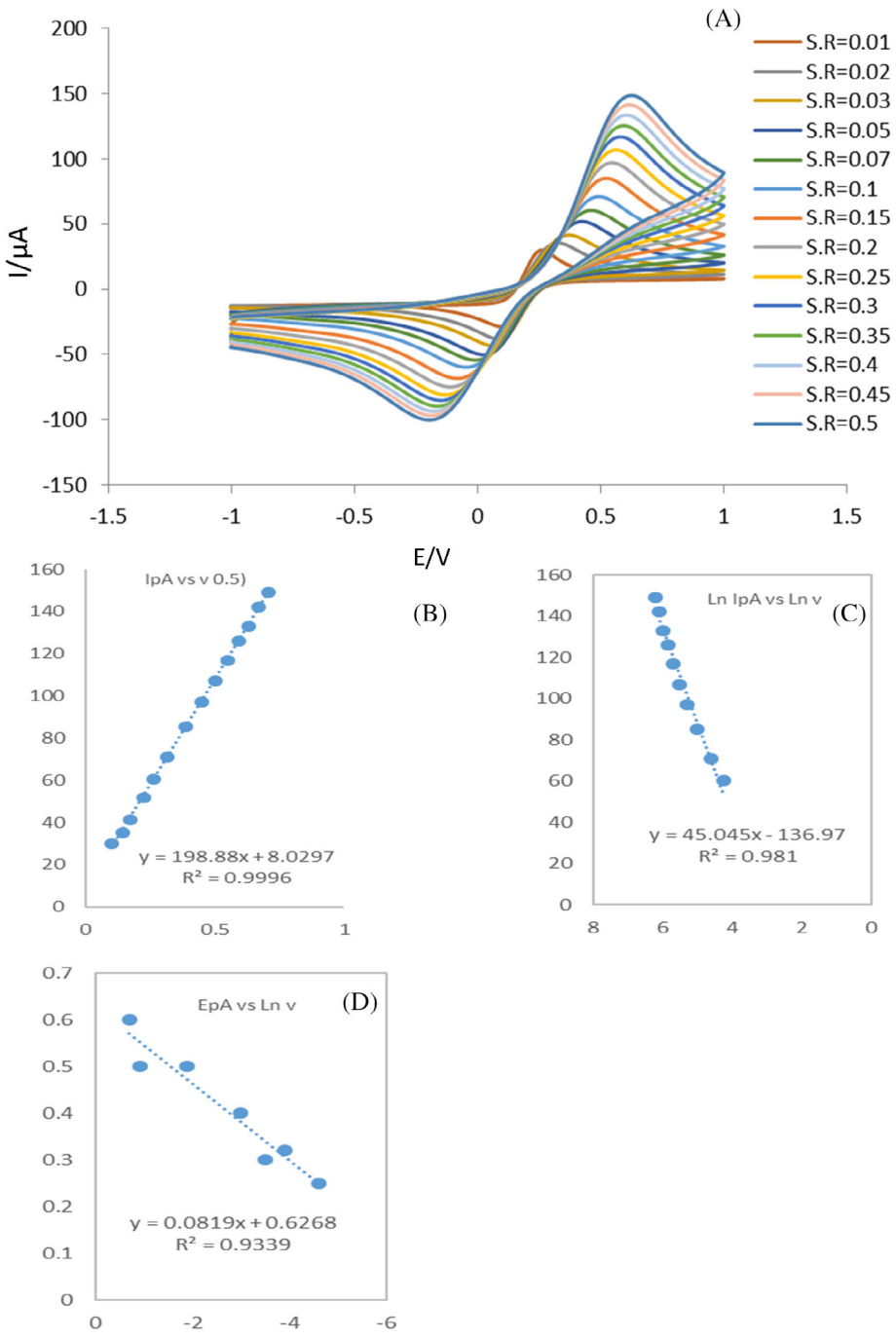

FIGURE 3 A, CVs of GCE electrode modified by AuNPs-CysA-GA. B, Dependency of oxidation peak currents variation sqaroroots of sweep rates. C, Varieties of Ln I_p vs Lnv. D, Variation of E_{pa} vs Lnv

between peak current and scan rate, useful information including the electrochemical reaction mechanism is obtained.

In order to examine the effect of scan rate, CVs of AuNPs-CysA-GA/GCE was recorded in different sweep rates in the range of 10 to 500 mV/s in 1 mM $[Fe(CN)_6]^{3-/4-}$ solutions (Figure 3A). Given the linear relationship between scan rate and peak current, it can be concluded that the electro oxidation procedure is controlled by the diffusion reaction.

The special surface coating of the GCE modified by AuNps-CysA-GA was calculated by studying the effect of sweep rates on the oxidation, peak current, and the response of the electrodes. As can be seen in Figure 3A-C, there is a linear relationship between, peak currents and sweep rates at low sweep rates, which indicates the catalytic nature of the modifier.

The specific surface coverage of the electrode is calculated using CVs technique by the following equation:

$$Ip = \left(F^2 n^2/4RT\right) \nu A\Gamma*$$

Γ^* is the surface coverage of the redox species, ν being the potential sweep rate, and A is the electrode surface area ($A = \pi r^2 = 0.0314$ cm^2).

The specially covered area of the GCE electrode modified by AuNPs-CysA-GA level is 67×10^{-9} mol/cm^2.

In addition using the variation of peak current vs square roots of sweep rate (Figure 3B), it is found the prepared interface (AuNPs-CysA-GA/GCE) show a diffusion process for the probe redox (Fe(III)/Fe (IV)) in 1 mM $[Fe(CN)_6]^{3-/4-}$ solutions.

These results were confirmed by Figure 3C. A slop close to 100 (1.00) for controlled processes with absorption and a gradient close to 50 (0.5) for controlled processes with diffusion. According to Figure 3C, mass transfer was of oxidation is controlled via diffusion process. Because the slop of chart is 45.045.

Also, Figure 3D shows the E_{pa} dependence to the Napierian logarithm of sweep rate (ln v). Given that in the irreversible reactions the E_{pa} is dependent of sweep rate, it can be concluded that the electron transfer in the electro oxidation reaction is irreversible. Considering the relation between the anodic peak potential to the Napierian logarithm of the potential sweep rate, the value of the electron transfer coefficient was obtained as 0.57.

3.3 | Analytical performance

The analytical behavior of the CEA immunosensor was investigated by DPV technique which has a better sensitivity compared with CV and SWV techniques. Figure 4A displays DPV responses of the immunosensor for different concentrations of CEA under optimal conditions in 1 mM $[Fe(CN)_6]^{3-/4}$.

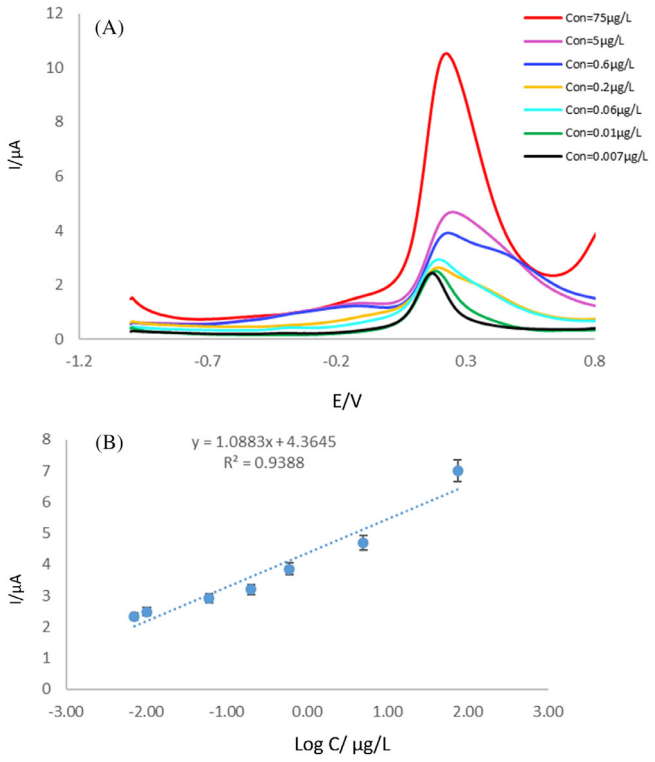

FIGURE 4 A, DPVs responses of the immunosensor for different concentrations of CEA: 0.007-5 µg/L in 1 mM of $Fe(CN)_6^{-3/-4}$. B, Calibration curve

Also, Figure 6B shows the corresponding calibration curve. There is a direct relationship between the peak current intensity and the natural logarithm of species concentration. The slope of the diagram was 1.08 which is the same as the sensitivity of the immunosensor and the proposed method. Also, the correlation coefficient was 0.9 which is acceptable.

As shown in DPV results, well-defined peak was clearly generated in the range from 0.007 to 5 µg/L, which were proportional to the concentrations of CEA. The linear regression equation is:

I (µA) = 1.0883 (CEA) + 4.3645 (R^2 = 0.9388) from concentration rang of 0.007 to 5 µg/L.

Also, the low limit of quantification (LLOQ) is calculated to be ~0.007 µg/L.

Compared with other immunosensors reported by analytical studies (Table 1),[46-57,62] the developed immunosensor showed better analytical performance in view of the linear range and the limit of detection. Efficient function of this sensor can be due to unique structure and unique electrical behavior of AuNPs, which lead to sensing of CEA in ng/ml concentration. Also, high surface area of interface (AuNPs-CysA-GA) for dense loading of Ab1 local to excellent sensitivity of the engineered immunosensor.

3.3.1 | Real sample analysis

According to the obtained results in detection of CEA in standard samples, the relevant sensor and proposed method can also be evaluated in real samples. Therefore, DPV technique was recorded at different concentrations of CEA in human plasma samples.

The CEA biomarker detection in human plasma sample was done by DPVs technique. The DPVs (Figure 5) show that the engineered immunosensor can discover the biomarker in a concentration range of 0.007-2 µg/L at the human plasma sample and regression equation is as follows:

$$I(\mu A) = 1.8419\,(CEA) + 7.4947, R^2 = 0.877.$$

The corresponding peak is related to the formation of immune-complexes and the evaluation of the effect of concentration can be accurately followed up at different antigen concentrations. On the other hand, the calibration curve obtained in the human plasma sample shows a linear relationship between the peak current intensity and the natural logarithm of the concentration. The sensitivity of the method was 1.84.

So the developed immunosensor was successfully used for detection of CEA in real samples.

3.4 | Stability study

The stability of the sensor was investigated by the DPV and SWV technique in the potential range of −1 to +1 V and after test, the sensor kept at a temperature of 4°C.

TABLE 1 Comparison of the analytical results for the biosensing of CEA using different methods

Method	Material	Dynamic range (ng/mL)	LOD (ng/mL)	Refs.
Polarization	Optical quantum weak measurements/Dopamine	5-50 μg/mL	0.749 μg/mL	46
Fluorescent	Magnetoelastic /Gold nanoparticles	0.1-100 ng/mL	2.5 pg/mL	47
Fluorescence	Copper nanocluster	0.01-2 ng/mL	0.0065 ng/mL	48
Electrochemical	Immunosensor /Cu_2O-gold	0.002-20 ng/mL	0.0002 ng/mL	49
Electrochemical	Potentiometric aptasensor/graphene oxide	0.01-100 ng/mL	9.4 pg/mL	50
Electrochemical	Immunosensor/Ferrocene	0.05-20 ng/mL	0.01 ng/mL	51
SPR	z-potential (Zpot)/gold Nanoparticles	0.1-2.5 ng/mL	17.8 ng/mL	52
Electrochemistry	Aptamer modified gold nanorod	0.0001-10 pg	0.05 pg/mL	53
Fluorescent	(MoS_2) nanosheets and aptamer	100 pg/mL-100 ng/mL	34 pg/mL	54
ECL	Aptasensor using Ag-PAMAM NCs	0.001-500 ng/mL	0.39 pg/mL cathode 0.20 pg/mL anode	55
ECL	Aptasensor/Au-CdS nanocomposites	0.0008-4 ng/mL	0.28 pg/mL	56
ECL	Gold/Cerium oxide nanoparticles	0.05-100 ng/mL	0.02 ng/mL	57
ECL	AuNPs/NB-ERGO/GCE	0.001-40 ng/mL	0.00045 ng/mL	59
Microconcentric nebulizer (MCN)-ICP-MS)	Magnetic nanoparticles (MNPs)	0.1-50 ng/mL	0.041 ng/mL	58
ETV-ICP-MS	Iminodiacetic acid modified silica coated magnetic nanoparticles (IDA-SCMNPs)	0.2-50 μg/L	0.058 μg/L	59
ICPMS	Eu^{3+}-labeled CEA antibody	0-500 ng/mL	0.14 ng/mL	60
ICPMS	AuNPs/ZnSe QDs/AgNPs	0.02-100 ng/mL	0.006 ng/mL	61
Electrochemistry	AuNPs /GCE	0.001-75 μg/mL	0.007 μg/mL	This work

Figure 6 shows the sensor has low stability after 2 days because the resulting current intensity has decreased. Therefore, it can be used as a single-use sensor.

3.5 | Selectivity of engineered immunosensor

To evaluate the specificity of the developed immunosensor for the accurate determination of CEA biomarker, several interferential

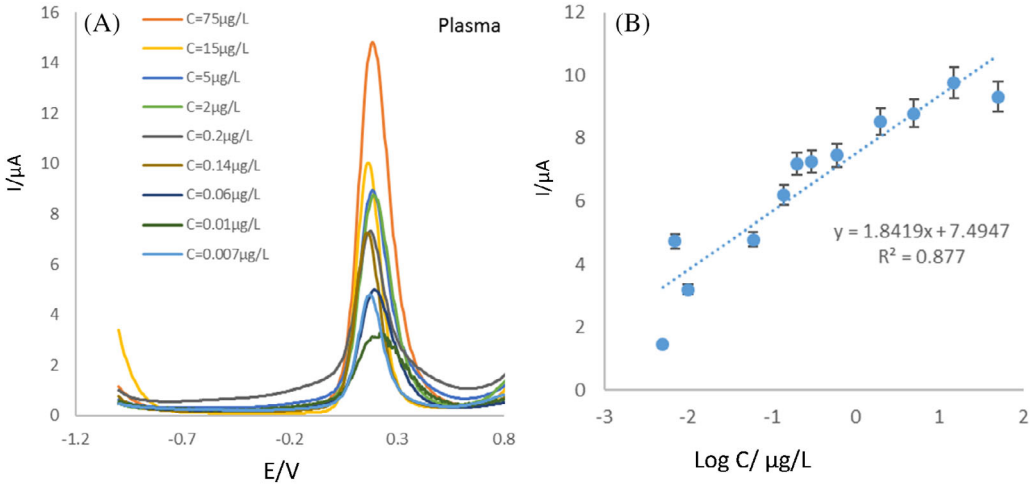

FIGURE 5 A, DPVs of the engineered immunosensor for the detection of CEA biomarker in the concentration range of 2-0.007 μg/L in human plasma samples. B, Calibration curve

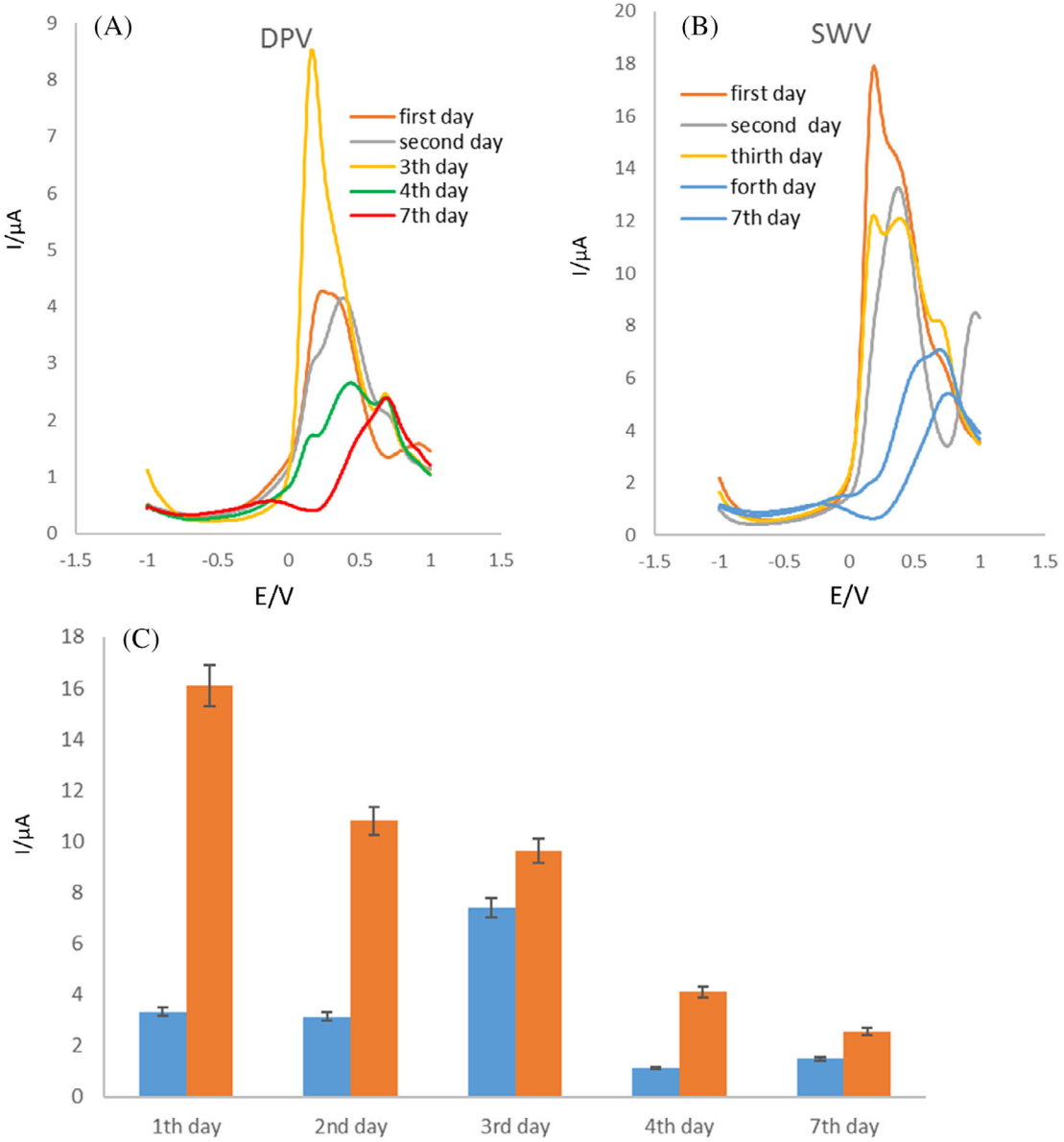

FIGURE 6 A, DPVs and B, SWVs and C, histograms for the stability study of AuNPs-CysA-GA/Ab1/BSA/CEA/Ab2 in the potential range of −1 to 1 V and sweep 50 mV/s in 1 mM of Fe $(CN)_6^{-3/-4}$ periodic time (168 hours)

species in real human samples such as BSA, PSA, CA125 and, CA 15.3, as serum proteins were investigated by DPV technique in 1 mM of Fe $(CN)_6^{-3/-4}$ as mediator solution. As can be seen in Figure 7, the peak location does not change and only the peak current intensity changes. The results show that there is little interference by the above proteins in the function of the relevant immunosensor.

4 | CONCLUSION

In summary, a novel sandwich-type immunosensor was successfully designed to the detection of CEA biomarker in a human plasma sample. For this purpose, AuNPs were used for the preparation of the substrate. The electrochemical immunoassay can identify and determine the CEA at low concentrations of this biomarkers in a human plasma sample. Under the optimized conditions, the LLOQ for the proposed immunosensor was recorded as 0.007 μg/L, which this evaluation was also performed at high linear range of 0.001-5 μg/L. The high performance of the proposed immunosensor is due to an increase in active surface area, high electrical conductivity, fast electron transfer, good catalytic properties, and optimal biocompatibility. All of these features indicate that the engineered immunosensor can be used as a multipurpose transducer for other biomarkers and is capable of being used in clinical and biomedical diagnosis.

ACKNOWLEDGEMENT

This work has been supported by Tabriz University of Medical Science.

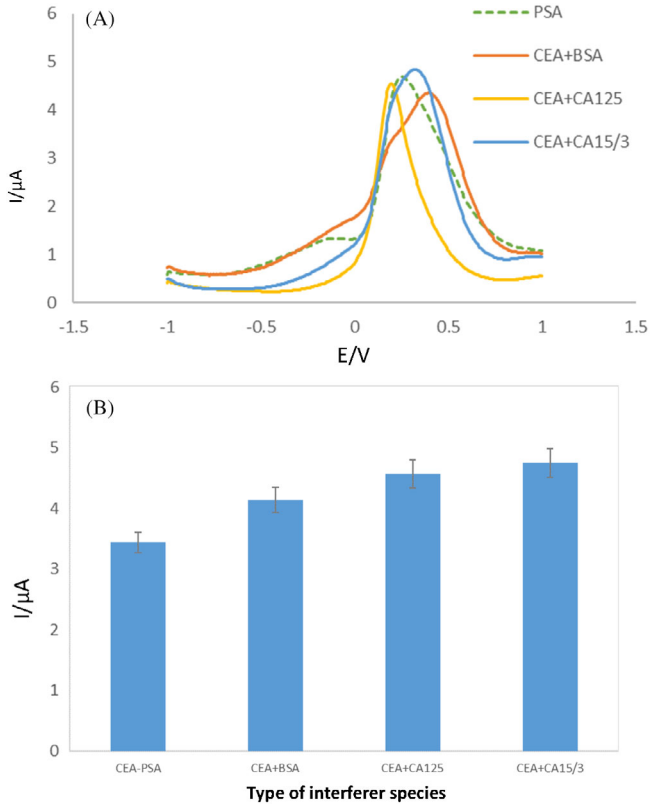

FIGURE 7 A, DPVs of the AuNPs-CysA-GA/Ab1/BSA/CEA/Ab2 in the presence of some serum proteins (BSA, CA15.3, CA125 and PSA). B, Histogram of peak currents vs type of interfering species

CONFLICT OF INTEREST

All the authors (M. Moradkhani, F. Farshchi, M. Hasanzadeh, A. Mokhtarzadeh) have read, approved, and made substantial contributions for the manuscript. None of the original material contained in this manuscript has been previously published nor is currently under review for publication elsewhere. Besides, authors declare no conflict of interests and/or commercial products or companies.

ORCID

Mohammad Hasanzadeh https://orcid.org/0000-0003-4918-1239

REFERENCES

1. Senkus E, Kyriakides S, Ohno S, Penault-Llorca F, Poortmans P, Rutgers E, Zackrisson S, Cardoso F. *Primary breast cancer: ESMO Clinical Practice Guidelines fordiagnosis, treatment and follow-up*. Ann Oncol. 2015;5:v8-30.
2. Agrawal P, Agrawal G, Shah A. *A thigh swelling, neoplasm or surprise?* Indian Pract. 2018;71(6):34-37.
3. Anand P, Kunnumakara AB, Sundaram C, et al. *Cancer is a preventable disease that requires major lifestyle changes*. Pharm Res. 2008;25(9): 2097-2116.
4. Hamadeh IS, Patel JN, Rusin S, Tan AR. *Personalizing aromatase inhibitor therapy in patients with breast cancer*. Cancer Treat Rev. 2018;70: 47-55.
5. Qiu Z, Shu J, Tang D. *Near-infrared-to-ultraviolet light-mediated photoelectrochemical aptasensing platform for cancer biomarker based on core–shell $NaYF_4$:Yb, Tm@TiO_2 upconversion microrods*. Anal Chem. 2017;90(1):1021-1028.
6. Kushi LH, Doyle C, McCullough M, et al. *American Cancer Society Guidelines on nutrition and physical activity for cancer prevention: reducing the risk of cancer with healthy food choices and physical activity*. CA Cancer J Clin. 2012;62(1):30-67.
7. Farshchi F, Hasanzadeh M, Solhi E. *Immunosensing of prostate cancer in human plasma samples using immobilization of antibody on the surface of mesoporous silica modified silver nanoparticles and its immunocomplex with prostate specific antigen*. Anal Methods. 2019;11:6159-6167.
8. Han K-q, Huang G, Gao C-f, et al. *Identification of lung cancer patients by serum protein profiling using surface-enhanced laser desorption/ionization time-of-flight mass spectrometry*. Am J Clin Oncol. 2008;31(2):133-139.
9. Shi G-F, Cao J-T, Zhang J-J, et al. *Aptasensor based on tripetalous cadmium sulfide-graphene electrochemiluminescence for the detection of carcinoembryonic antigen*. Analyst. 2014;139(22):5827-5834.
10. Valencakova-Agyagosova A, Frischova Z, Sevcikova Z, et al. *Determination of carcinoembryonic antigen and cancer antigen (CA 15-3) in bitches with tumours on mammary gland: preliminary report*. Vet Comp Oncol. 2014;12(3):205-214.
11. Liu F, Zhang H, Wu Z, et al. *Highly sensitive and selective lateral flow immunoassay based on magnetic nanoparticles for quantitative detection of carcinoembryonic antigen*. Talanta. 2016;161:205-210.
12. Huang Z, Wu S, Duan N, Hua D, Hu Y, Wang Z. *Sensitive detection of carcinoembryonic antigen with magnetic nano-bead and upconversion nanoparticles-based immunoassay*. J Pharm Biomed Anal. 2012;66: 225-231.
13. Li S-X, Yang Y-Q, Jin L-J, Cai Z-G, Sun Z. *Detection of survivin, carcinoembryonic antigen and ErbB2 level in oral squamous cell carcinoma patients*. Cancer Biomark. 2016;17(4):377-382.
14. Li R, Feng F, Chen Z-Z, et al. *Sensitive detection of carcinoembryonic antigen using surface plasmon resonance biosensor with gold nanoparticles signal amplification*. Talanta. 2015;140:143-149.
15. Martínez-Mancera FD, García-López P, Hernández-López JL. *Preclinical validation study of a miniaturized electrochemical immunoassay based on square wave voltammetry for early detection of carcinoembryonic antigen in human serum*. Clin Chim Acta. 2015;444: 199-205.
16. Tian J, Zhou L, Zhao Y, et al. *The application of CdTe/CdS in the detection of carcinoembryonic antigen by fluorescence polarization immunoassay*. J Fluoresc. 2012;22(6):1571-1579.
17. Wu D, Ma H, Zhang Y, Jia H, Yan T, Wei Q. *Corallite-like magnetic Fe_3O_4@MnO_2@Pt nanocomposites as multiple signal amplifiers for the detection of carcinoembryonic antigen*. ACS Appl Mater Interfaces. 2015;7(33):18786-18793.
18. Zhu K, Zhang Y, Li Z, et al. *Simultaneous detection of α-fetoprotein and carcinoembryonic antigen based on Si nanowire field-effect transistors*. Sensors. 2015;15(8):19225-19236.
19. Mao L, Liua Y, Yang S, Li Y, Zhang X, Wei Y. *Recent advances and progress of fluorescent bio-/chemosensors based on aggregation-induced emission molecules*. Dyes Pigm. 2019;162:611-623.
20. Wan Q, Huang Q, Liu M, Xu D, Zhang X, Wei Y. *Aggregation-induced emission active luminescent polymeric nanoparticles: non-covalent fabrication methodologies and biomedical applications*. Appl Mater Today. 2017;9:145-160.
21. Jiang R, Liu H, Liu M, Tian J, Zhang X, Wei Y. *A facile one-pot Mannich reaction for the construction of fluorescent polymeric nanoparticles with aggregation-induced emission feature and their biological imaging*. Mater Sci Eng C. 2017;81:416-421.

22. Long Z, Mao L, Liu M, et al. *Marrying multicomponent reactions and aggregation-induced emission (AIE): new directions for fluorescent nanoprobes*. Polym. Chem. 2017;8:5644-5654.
23. Zhang X, Zhang X, Yang B, et al. *Fabrication of aggregation induced emission dye-based fluorescent organic nanoparticles via emulsion polymerization and their cell imaging applications*. Polym Chem. 2014;5: 399-404.
24. Jiang R, Liu M, Chen T, Huang H, Zhang X, Wei Y. *Facile construction and biological imaging of cross-linked fluorescent organic nanoparticles with aggregation-induced emission feature through a catalyst-free azide-alkyne click reaction*. Dyes Pigm. 2018;148:52-60.
25. Yang Z, Liu H, Liu D. *Spatial regulation of synthetic and biological nanoparticles by DNA nanotechnology*. NPG Asia Mater. 2015;7(2): e161.
26. Grzelczak M, Pérez-Juste J, Mulvaney P, Liz-Marzán LM. *Shape control in gold nanoparticle synthesis*. Chem Soc Rev. 2008;37(9):1783-1791.
27. Lévy R, Thanh NT, Doty RC, et al. *Rational and combinatorial design of peptide capping ligands for gold nanoparticles*. J Am Chem Soc. 2004; 126(32):10076-10084.
28. Selvaraju T, Das J, Jo K, et al. *Nanocatalyst-based assay using DNA-conjugated Au nanoparticles for electrochemical DNA detection*. Langmuir. 2008;24(17):9883-9888.
29. Ye P, Xu Z-K, Wu J, Innocent C, Seta P. *Nanofibrous membranes containing reactive groups: electrospinning from poly (acrylonitrile-co-maleic acid) for lipase immobilization*. Macromolecules. 2006;39(3):1041-1045.
30. Liu M, Zeng G, Wang K, et al. *Recent developments in polydopamine: an emerging soft matter for surface modification and biomedical applications*. Nanoscale. 2016;8(38):16819-16840.
31. Zhang X, Huang Q, Liu M, Tian J, Zhang X, Wei Y. *Preparation of amine functionalized carbon nanotubes via a bioinspired strategy and their application in Cu^{2+} removal*. Appl Surf Sci. 2015;343:19-27.
32. Liu M, Ji J, Zhang X, et al. *Self-polymerization of dopamine and polyethyleneimine: novel fluorescent organic nanoprobes for biological imaging applications*. J Mater Chem B. 2015;3:3476-3482.
33. Huang L, Liu M, Huang H, Wen Y, Zhang X, Wei Y. *Recent advances and progress on melanin-like materials and their biomedical applications*. Biomacromolecules. 2018;19(6):1858-1868.
34. Huang Q, Liu M, Chen J, Wan Q, Zhang X, Wei Y. *Facile preparation of MoS_2 based polymer composites via mussel inspired chemistry and their high efficiency for removal of organic dyes*. Appl Surf Sci. 2017;419: 35-44.
35. Huang Q, Liu M, Mao L, et al. *Surface functionalized SiO_2 nanoparticles with cationic polymers via the combination of mussel inspired chemistry and surface initiated atom transfer radical polymerization: characterization and enhanced removal of organic dye*. J Colloid Interface Sci. 2017; 499:170-179.
36. Zhang X, Huang Q, Deng F, Huang H, Wei Y. *Mussel-inspired fabrication of functional materials and their environmental applications: progress and prospects*. Appl Mater Today. 2017;7:222-238.
37. Liu Y, Ai K, Lu L. *Polydopamine and its derivative materials: synthesis and promising applications in energy, environmental, and biomedical fields*. Chem. Rev. 2014;114(9):5057-5115.
38. Zeng G, Huang L, Huang Q, Liu M, Zhang X, Wei Y. *Rapid synthesis of MoS_2-PDA-Ag nanocomposites as heterogeneous catalysts and antimicrobial agents via microwave irradiation*. Appl Surf Sci. 2018;459: 588-595.
39. Huang Q, Liu M, Zhao J, Chen J, Zhang X, Wei Y. *Facile preparation of polyethylenimine-tannins coated SiO_2 hybrid materials for Cu^{2+} removal*. Appl Surf Sci. 2018;427:535-544.
40. Gan D, Huang Q, Dou J, Huang H, Zhang X, Wei Y. *Bioinspired functionalization of MXenes ($Ti_3C_2T_X$) with amino acids for efficient removal of heavy metal ions*. Appl Surf Sci. 2020;504:144603.
41. Dong H, Meng X, Dai W, et al. *Highly sensitive and selective microRNA detection based on DNA-bio-bar-code and enzyme-assisted strand cycle exponential signal amplification*. Anal Chem. 2015;87(8): 4334-4340.
42. Braun M, Hessamian-Alinejad A, de Lacroix B, Alvarez B, Fischer G. *Novel spiroannulated 3-benzofuranones. Synthesis and inhibition of the human peptidyl prolyl cis/trans isomerase Pin1*. Molecules. 2008;13(4): 995-1003.
43. Sharma R, Kodavanti UP, Smith LL, Mehendale HM. *The uptake and metabolism of cystamine and taurine by isolated perfused rat and rabbit lungs*. Int J Biochem Cell Biol. 1995;27(7):655-664.
44. Favre HA, Powell WH. *Nomenclature of Organic Chemistry: IUPAC Recommendations and Preferred Names 2013*. UK: Royal Society of Chemistry; 2013.
45. Morris JK. *A formaldehyde glutaraldehyde fixative of high osmolality for use in electron microscopy*. J Cell Biol. 1965;27:1A-149A.
46. He Y, Xie S, Yang X, Yuan R, Chai Y. *Electrochemical peptide biosensor based on in situ silver deposition for detection of prostate specific antigen*. ACS Appl Mater Interfaces. 2015;7(24):13360-13366.
47. Bazhan E, Baradaran B. *MicroRNA-143 inhibits migration of human prostate cancer cells (PC3)*. J Ardabil Univ Med Sci. 2017;17(2): 142-153.
48. Jang HD, Kim SK, Chang H, Choi JW. *3D label-free prostate specific antigen (PSA) immunosensor based on graphene–gold composites*. Biosens Bioelectron. 2015;63:546-551.
49. Baradaran A, Mahmoud R-KM. *Histopathological study of the combination of metformin and garlic juice for the attenuation of gentamicin renal toxicity in rats*. J Renal Inj Prev. 2012;2(1):15-21.
50. Liu J, Lu CY, Zhou H, Xu JJ, Wang ZH, Chen HY. *A dual-functional electrochemical biosensor for the detection of prostate specific antigen and telomerase activity*. Chem Commun. 2013;49 (59):6602-6604.
51. Sonnenschein C, Soto AM. *Theories of carcinogenesis: an emerging perspective*. Semin Cancer Biol. 2008;18(5): 372-377.
52. Wu G, Datar RH, Hansen KM, Thundat T, Cote RJ, Majumdar A. *Bioassay of prostate-specific antigen (PSA) using microcantilevers*. Nat Biotechnol. 2001;19(9):856-860.
53. Kong R-M, Ding L, Wang Z, You J, Qu F. *A novel aptamer-functionalized MoS_2 nanosheet fluorescent biosensor for sensitive detection of prostate specific antigen*. Anal Bioanal Chem. 2015;407(2): 369-377.
54. Soukka T, Antonen K, Härmä H, Pelkkikangas AM, Huhtinen P, Lövgren T. *Highly sensitive immunoassay of free prostate-specific antigen in serum using europium(III) nanoparticle label technology*. Clin Chim Acta. 2003;328(1-2):45-58.
55. Qi H, Li M, Dong M, Ruan S, Gao Q, Zhang C. *Electrogenerated chemiluminescence peptide-based biosensor for the determination of prostate-specific antigen based on target-induced cleavage of peptide*. Anal Chem. 2014;86(3):1372-1379.
56. Wu Z, Fu Q, Yu S, et al. *Pt@AuNPs integrated quantitative capillary-based biosensors for point-of-care testing application*. Biosens Bioelectron. 2016;85:657-663.
57. Catalona WJ. *History of the discovery and clinical translation of prostate-specific antigen*. Asian J Urol. 2014;1(1):12-14.
58. Peng H, Chen B, He M, Zhang Y, Hu B. *Magnetic quantitative immunoanalysis of carcinoembryonic antigen by ICP-MS with mercury labels*. J Anal At Spectrom. 2011;26:1217-1223.
59. Chen B, Hu B, Jiang P, He M, Peng H, Zhang X. *Nanoparticle labelling-based magnetic immunoassay on chip combined with electrothermal vaporization-inductively coupled plasma mass spectrometry for the determination of carcinoembryonic antigen in human serum*. Analyst. 2011;136(19):3934-3942.
60. Hu S, Zhang S, Hu Z, Xing Z, Zhang X. *Detection of multiple proteins on one spot by laser ablation inductively coupled plasma mass spectrometry*

and application to immuno- microarray with element-tagged antibodies. Anal Chem. 2007;79(3):923-929.
61. Cao Y, Feng J, Tang L, Mo G, Mo W, Deng B. *Detection of three tumor biomarkers in human lung cancer serum using single particle inductively coupled plasma mass spectrometry combined with magnetic immunoassay*. Spectrochim. Acta, Part B. 2020; 166:105797.
62. Rebelo TS, Santos C, Costa-Rodrigues J, et al. *Novel Prostate SpecificAntigen plastic antibody designed with charged binding sites for an improved protein binding and its application in a biosensor of potentiometric transduction*. Electrochim Acta. 2014;132: 142-150.

SUPPORTING INFORMATION

Additional supporting information may be found online in the Supporting Information section at the end of this article.

How to cite this article: Moradkhani M, Farshchi F, Hasanzadeh M, Mokhtarzadeh A. A novel bioassay for the monitoring of carcinoembryonic antigen in human biofluid using polymeric interface and immunosensing method. *J Mol Recognit*. 2020;e2852. https://doi.org/10.1002/jmr.2852